DOI: https://doi.org/10.68732/204eceafe4b81639

ISBN: 978-9989-2053-7-8

Study on time-dependent deformation surrogate model for Reservoir Bank Slope Considering Water Effects

C. Y. Wei, C. F. Gao, S. Y. Yue, D. H. Yu, Z. Y. Pang & Y. R. Liu
Tsinghua Universtity, State Key Laboratory of Hydroscience and Engineering, Beijing, China
liuyaoru@tsinghua.edu.cn
0000-0001-6703-6604

Abstract

Numerical simulation has proven effective for evaluating slope stability, its computational cost becomes a bottleneck when repeated model calls are required in engineering analyses. Surrogate models offer a practical alternative. This paper presents a deep learning-based surrogate model for time-dependent deformation prediction of reservoir bank slopes. The deformation process is simulated using an elastic-viscoplastic creep constitutive model that accounts for water effects. A dataset was constructed by generating 7490 sets of mechanical parameters via Latin hypercube sampling and computing the corresponding slope deformations at monitoring points. A neural network framework combining multi-layer stacked GRUs (gated recurrent units) and fully connected layers was developed to capture the complex nonlinear relationship between rock mass parameters and slope time-dependent deformation. Results demonstrate that the surrogate model achieves a coefficient of determination $R^2 > 0.97$ in predicting time-dependent slope deformation. Given a set of mechanical parameters, it can rapidly output the corresponding deformation, thereby providing a reliable basis for the analysis and calculation of rock slopes.

Keywords

Mechanical parameters inversion, Deep learning Ggenetic algorithm, Surrogate model, Reservoir bank slope.

1 Introduction

The destabilization of reservoir bank slopes poses a serious threat to the safety of hydraulic structures and may lead to substantial property losses and casualties (Chen et al. 2001; Lyu et al. 2025). Therefore, accurate stability assessment is crucial in the design and operational management of such engineering projects. Numerical simulation has become an effective tool for evaluating slope stability (Song et al. 2019). However, its computational efficiency remains a significant bottleneck in analyses requiring repeated model calls (Zhong et al. 2025; Qiu et al. 2018). To address this issue, surrogate models have been introduced as an efficient alternative, offering considerably lower computational cost while maintaining acceptable accuracy, thereby greatly enhancing the efficiency of slope stability analyses (Song et al. 2023).

Traditional methods for constructing surrogate models include the response surface method (Kasama et al. 2023), polynomial chaos expansion (Chehade et al. 2023), and Kriging method (Cabanzo et al, 2023). For instance, Dadashzadeh et al. (2017) employed a response surface approach for reliability-based slope stability analysis and reported a 72% improvement in efficiency compared to Monte Carlo simulation. Liao et al. (2025) extended traditional polynomial chaos expansion by integrating bootstrap resampling with an active learning algorithm to adaptively select informative samples for surrogate model training. Zhang and Dias (2024) developed an adaptive polynomial chaos Kriging metamodel for efficient probabilistic slope analysis under seismic conditions, accounting for parameter uncertainties.

Traditional methods for constructing surrogate models are often limited by the curse of dimensionality and insufficient accuracy, and are primarily applicable to static elastoplastic analyses (Zhou et al. 2021). Relatively few studies have focused on developing time-dependent surrogate models based on creep constitutive models (Zhuang et al. 2025). For reservoir bank slopes, water-rock interaction is a critical factor driving continuous deformation under the influence of reservoir impoundment. To address these gaps, this paper proposes a deep learning-based surrogate model for predicting time-dependent deformation that accounts for water effects. First, numerical samples are generated using an elastic-viscoplastic creep model that incorporates the influence of water. Next, a surrogate model framework is constructed using a deep learning architecture combining multi-layer stacked GRUs and fully connected layers. Finally, the model is trained and its predictive performance is evaluated.

2 Methodology

2.1 Creep constitutive model considering water effects

In this study, creep behavior is simulated using a creep damage model grounded in the thermodynamics of internal variables (Zhang et al. 2014). This model introduces an internal variable χ to characterize the damage evolution resulting from microstructural changes during creep deformation. It effectively captures the three characteristic stages of slope creep: transitional creep, steady-state creep, and accelerated creep. The constitutive relationship is expressed as follows:

$$\dot{\boldsymbol{\varepsilon}} = \dot{\boldsymbol{\varepsilon}}^{e} + \dot{\boldsymbol{\varepsilon}}^{ve} + \dot{\boldsymbol{\varepsilon}}^{vp} \tag{1}$$

$$\dot{\boldsymbol{\varepsilon}}^{e} = \boldsymbol{C} : \dot{\boldsymbol{\sigma}} \tag{2}$$

$$\dot{\boldsymbol{\varepsilon}}^{ve} = \frac{\partial A}{\partial \boldsymbol{\sigma}} \dot{\gamma} + \frac{\partial}{\partial \chi}\left(\frac{\partial A}{\partial \boldsymbol{\sigma}} \gamma \right) \dot{\chi} \tag{3}$$

$$\dot{\boldsymbol{\varepsilon}}^{vp} = \frac{\partial P_i}{\partial \boldsymbol{\sigma}} \dot{\lambda}_i + \frac{\partial}{\partial \chi}\left(\frac{\partial P_i}{\partial \boldsymbol{\sigma}} \lambda_i \right) \dot{\chi} \tag{4}$$

where $\dot{\boldsymbol{\varepsilon}}^{e}$ is the elastic strain rate, $\dot{\boldsymbol{\varepsilon}}^{ve}$ is the viscoelastic strain rate, $\dot{\boldsymbol{\varepsilon}}^{vp}$ is the viscoplastic strain rate, $\boldsymbol{\sigma}$ is the stress tensor, $\boldsymbol{C}$ denotes the fourth-order compliance tensor, γ, λ, and χ are all internal variables, A and P_i are functions of $\boldsymbol{\sigma}$ and χ.

To account for the influence of water storage process, the model incorporates two main mechanisms. First, based on measured water-level data, seepage pressure is dynamically updated at each calculation step to accurately reflect pore water pressure effects. Second, the soaking duration of the corresponding rock mass is recorded during the computation, enabling real-time updates of key mechanical parameters—such as the friction coefficient (*f*), cohesion (*c*), and elastic modulus (*E*)—at every calculation step according to the following formulas.

$$D_f(t) = f_\infty + (1 - f_\infty)\ e^{-\lambda_f \cdot t} \tag{5}$$

$$D_c(t) = f_\infty / \eta + (1 - f_\infty / \eta)\ e^{-\lambda_f \cdot \eta \cdot t} \tag{6}$$

$$D_E(t) = E_\infty + (1 - E_\infty)\ e^{-\lambda_E \cdot t} \tag{7}$$

where f_∞ and E_∞ represent the normalized long-term strengths, while λ_f and λ_E denote the corresponding attenuation rates. η is adjustment factor ($\eta > 1.0$), ensuring that the degradation of cohesion is more pronounced than that of the friction coefficient.

2.2 Framework of time-dependent deformation surrogate model considering water effects

In this study, a neural network architecture is constructed using a deep learning framework that combines multi-layer stacked GRUs and fully connected layers. The network provides two separate input interfaces: one for time-series data (Input-I) and another for static parameters (Input-II). The GRU, a variant of recurrent neural networks, regulates information flow through its update and reset gates, effectively capturing short-term dependencies in sequential data and making it well-suited for time-series model (Yan et al. 2022). The fully connected layer serves as a fundamental component in neural networks, with each neuron connected to all outputs from the previous layer, enabling feature synthesis and nonlinear mapping (Ma et al. 2021). Input-I consists of time-dependent variables, including the water-induced degradation of rock mass mechanical parameters (*E*,*f*, *c*), along with the time series of reservoir waterlevel. Input-II comprises static creep parameters. The model outputs the timeseries of deformation at monitoring points (Fig. 1).

The Huber loss function is adopted for model training. This loss function applies a quadratic penalty for small errors, similar to the mean squared error, and transitions to a linear penalty for larger errors, thereby enhancing robustness against outliers.

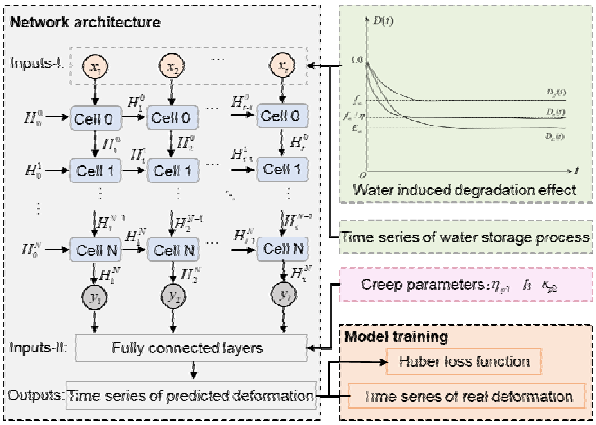


Fig. 1 Framework of time-dependent deformation surrogate model considering water effects.

3 Construction of data sets and model trraining

3.1 Numerical Sample Calculation

A reservoir bank slope in China is selected as the study object. The slope surface features alternating small gullies and ridges, with a platform located at the top. In the lower part of the deformation zone, altered rock zones are present. the mechanical properties of these rocks deteriorate significantly under prolonged water exposure, leading to ongoing slope deformation.

A computational model is established for a typical cross-section located in the midslope area, as illustrated in Fig. 2. The deformation zone is locally refined to enable detailed simulation while minimizing computational time. The model contains a total of 33,724 elements and 41,630 nodes.

As outlined in Section 2.1, the numerical method employed accounts for water-induced deterioration d during creep analysis. In this simulation, the mechanical parameter degradation of altered rock under water immersion is considered, governed by five degradation parameters in Eq. 5 ~ Eq. 7. The ranges of these degradation parameters and creep parameters are determined through trial simulations to ensure they encompass the actual slope deformation. Within these ranges, Latin hypercube sampling (uniform distribution) is applied to randomly generate 7,490 sets of rock mass mechanical parameters. Based on these parameter sets, deformation at five monitoring points (showed in Fig. 2) is calculated for the period from 2009/3/1 to 2024/8/21. Using a monthly time step (resulting in a time series length

of 187 steps), a dataset of 7,490 × 187 × 5 deformation values is obtained for subsequent surrogate model training.

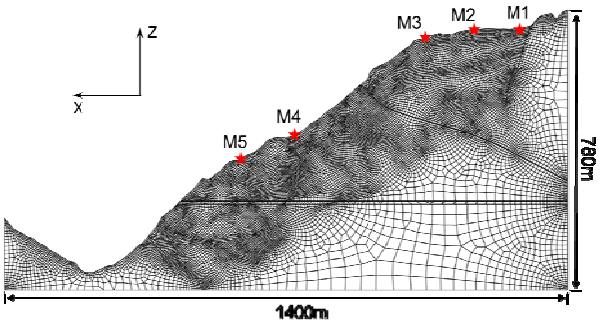


Fig. 2 Finite element mesh of the slope.

3.2 Model training and accuracy evaluation indicators

The numerical samples described above are formatted to match the model framework introduced in Section 2. Each sample consists of multiple time-series inputs and multiple static parameter inputs, with the exact number determined by the material partitions and the mechanical parameters defined in the numerical model.

Based on the numerical samples generated in Section 3.1, Each sample are normalized to ensure consistent scales across features. The dataset is split into training, validation, and test sets in an 8:1:1 ratio, corresponding to 5992, 749, and 749 samples, respectively.

Model performance is sensitive to hyperparameter settings; therefore, optimizing hyperparameters is essential to achieve the best surrogate model performance. The hyperparameters tuned in this study include training parameters (e.g., learning rate, batch size, and sample size), loss-function parameters (e.g., the Huber loss coefficient), and model architecture parameters (e.g., the number of hidden layers and the forgetting rate of each layer). Due to space limitations, the optimal hyperparameters identified for the case study are provided directly in Table 1.

Table 1. Optimal hyperparameters of the surrogate model.

Training	**loss function**	**Surrogate model architecture**
Learningrate(0.0014)	Huber threshold δ(0.92)	Neurons for each hidden layer (218,246,153,205)
Batch size(32)	-	Dropout ratio for each hidden layer (0.48,0.32,0.12,0.36)

4 Performance evaluation of the surrogate model

In contrast to the loss function, the evaluation metrics focus specifically on the prediction accuracy of the deformation time series, using the test set as the assessment basis. To objectively measure the performance of the surrogate model, three statistical indicators is determination coefficient (R^2).

$$R^2 = 1 - \sqrt{\frac{\sum_{n=1}^{N}\left\{\sum_{t=1}^{T}\sum_{m=1}^{M}[\hat{y}_m^{(t)} - y_m^{(t)}]^2\right\}}{\sum_{n=1}^{N}\left\{\sum_{t=1}^{T}\sum_{m=1}^{M}[y_m^{(t)}]^2\right\}}} \tag{8}$$

where N is the number of samples in the test set, M represents the number of time series groups in each sample, and T denotes the length of the time series. $\hat{y}_m^{(t)}$ and $y_m^{(t)}$ denote the predicted and true values of the time-series group in each sample. In this study, N=749, M=5, T=187.

Under the optimal hyperparameter configuration, the surrogate model was evaluated and achieved a coefficient of determination (R^2) of 0.9753 on the test set. The distribution of R^2 across the 749 samples in the test set is presented in Fig. 3. As shown, the R^2 values for the test samples range from 0.95 to 1.00. Only a small proportion of samples exhibit lower predictive accuracy: fewer than 5% have an R^2 below 0.98, and less than 1% fall below 0.96. These lower-accuracy samples are

predominantly edge cases, which are expected to have minimal impact on subsequent engineering applications.

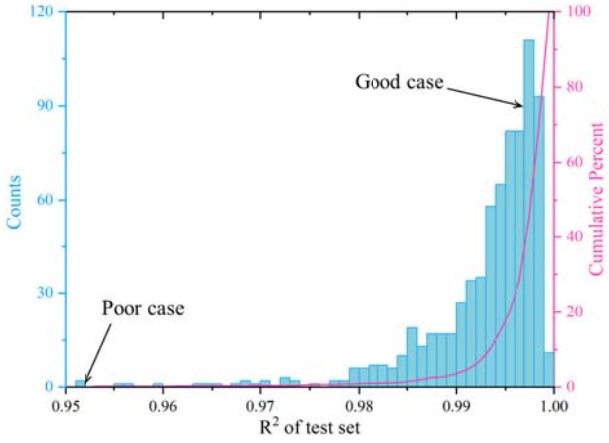


Fig. 3 The distribution of R^2 on the test set.

Two typical cases are selected, corresponding to different R^2 (0.95 and 0.99), to show the difference between the deformation time series predicted value and calculatedvalue. For better cases, the predicted value and the calculated value curve are almost completely coincident. For poor cases, there is a certain deviation between the test value and the calculated value, especially the measuring points of M3, but the deformation law is basically the same (Fig. 4).

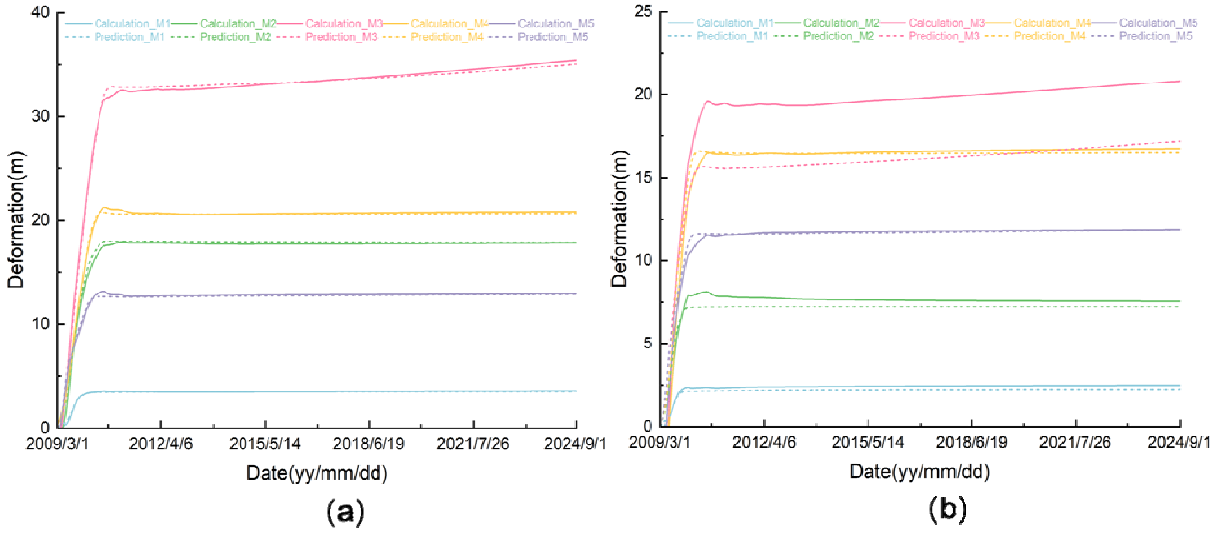


Fig. 4 Comparison of predicted and calculated values of deformation: (a) Good case; (b) Poor case.

In summary, the developed surrogate model accurately predicts the deformation time series at slope monitoring points. Given a set of mechanical parameters, it can rapidly output the corresponding deformation, thereby providing a reliable basis for the analysis and calculation of rockslopes.

5 Conclusion

This study developed a deep learning-based surrogate model for predicting time-dependent deformation of a reservoir bank slope and applied it to a practical engineering case. The main conclusions are as follows:

(1) By integrating multi-layer stacked GRUs and fully connected layers, the proposed surrogate model simultaneously processes time series inputs (such as the impoundment process and water-induced rock mass degradation) and static mechanical parameters.

(2) The model successfully captures the complex nonlinear relationship between mechanical parameters and slope deformation at monitoring points, achieving a prediction accuracy of $R^2 > 0.97$ on the test set, which satisfies the requirements for engineering applications.

Acknowledgements

This study was supported by the National Natural Science Foundation of China with Grant No. 41961134032.

References

Chen ZY, Wang XG, Haberfield C, Yin JH, Wang YJ (2001) A three-dimensional slope stability analysis method using the upper bound theorem - Part I: theory and methods.International journal of rock mechanics and mining sciences 38(3): 369-378.https://doi.org/10.1016/S1365-1609(01)00012-0.

Lyu QC, Liu T, Bai JL, Zhang Q, Wei CY, Liu YR. (2025) Study on deformation mechanism of reservoir slope near dam during operation period. American Rock Mechanics Association,Santa Fe, New Mexico, USA, 8 June 2025.

Song DQ, Che AL, Zhu RJ,Ge XR. (2019) Natural frequency characteristics of rock masses containing a complex geological structure and their effects on the dynamic stability of slopes. Rock mechanics and rock Engineering 52(11):4457-4473.https://doi.org/10.1007/s00603-019-01885-7.

Zhong K, Tan XH, Liu SW, Lu ZT, Hou XL, Wang Q. (2025) Prediction of slope failure probability based on machine learning with genetic-ADASYN algorithm. Engineering Geology 346:107885.https://doi.org/10.1016/j.enggeo.2024.107885.

Qiu XY, Chen JY, Shi XZ, Zhang S, Zhou J, Chen X. (2018) Deformation prediction and analysis of underground mining during stacking of dry gangue in open-pit based on response surface methodology. Journal of central south university25(2):406-417.https://doi.org/10.1007/s11771-018-3746-3.

Song JT, Yuan S, Xu ZG, Li XR. (2023) Fast inversion method for seepage parameters of core earth-rock dam based on LHS-SSA-MKELM fusion surrogate model. Structures 55:160-168.https://doi.org/10.1016/j.istruc.2023.06.049.

Kasama K, Furukawa Z, Hu LH. (2021) Practical reliability analysis for earthquake-induced 3D landslide using stochastic response surface method. Computers and geotechnics137:104303.https://doi.org/10.1016/j.compgeo.2021.104303.

Chehade HA, Guo X, Dias D, Sadek M, Jenck O, Chehade FH. (2023) Reliability analysis for internal seismic stability of geosynthetic-reinforced soil walls. Geosynthetics international 30(3): 296-314.https://doi.org/10.1680/jgein.22.00250.

Cabanzo CM, Tinoco J, Sousa HS, Coelho M, Matos JC. (2023) Adaptation of traditional risk-based methodology for slopes to probabilistic-based approach integrating surrogate models. Computers and geotechnics. 161:105577.https://doi.org/10.1016/j.compgeo.2023.105577.

Dadashzadeh N, Duzgun HSB, Yesiloglu-Gultekin N. (2017) Reliability-Based Stability Analysis of Rock Slopes Using Numerical Analysis and Response Surface Method. Rock mechanics and rock engineering50(8):2119-2133.https://doi.org/10.1007/s00603-017-1206-2.

Liao K, Zhao XY, Wu YP, Miao FS, Pan YT, Beer M. (2025) Efficient reliability analysis of slopes in spatially variable soils with active learning-assisted bootstrap polynomial chaos expansion. Computers and geotechnics 179:107022.https://doi.org/10.1016/j.compgeo.2024.107022.

Zhang TT, Dias D. (2024) An efficient solution for probabilistic slope seismic stability analysis based on polynomial chao kriging metamodel. Geohazards5(2):530-546.https://doi.org/10.3390/geohazards5020027.

Zhou Z, Li DQ, Xiao T, Gao ZJ, Du WQ. (2021) Response surface guided adaptive slope reliability analysis in spatially varying soils. Computers and geotechnics132:103966.https://doi.org/10.1016/j.compgeo.2020.103966.

Zhuang WY, Liu YR, Zhang K, Lyv QC, Hou SK, Yang Q. (2025) A physics knowledge-based surrogate model framework for timedependent slope deformation: Considering water effect and sliding states. Journal of rock mechanics and geotechnical engineering 17(9):5416-5436.https://doi.org/10.1016/j.jrmge.2024.11.002.

Zhang L, Liu YR, Yang Q. (2014) A creep model with damage based on internal variable theory and its fundamental properties.Mechanics of materials78:44-55.https://doi.org/10.1016/j.mechmat.2014.07.017.

Yan MT, Zhang ZM, Gao SC, Cao SY. (2022) Predicting aerodynamic pressure on a square cylinder from wake velocity field by masked gated recurrent unit model. Physics of fluids 34:115101.https://doi.org/10.1063/5.0110491.

Ma L, Huang C, Liu ZS, Morin KA, Aziz M, Meints C. (2021) The correlation between drainage chemistry and weather for full-scale waste rock piles based on artificial neural network. Journal of contaminant hydrology239:103793.https://doi.org/10.1016/j.jconhyd.2021.103793.